



Published in final edited form as:

Curr Biol. 2010 August 10; 20(15): 1383–1388. doi:10.1016/j.cub.2010.06.022.

Determinants of divergent adaptation and Dobzhansky-Muller interaction in experimental yeast populations

James B. Anderson^{1,6}, Jason Funt^{2,3,6}, Dawn Anne Thompson³, Snehit Prabhu³, Amanda Socha³, Caroline Sirjusingh¹, Jeremy R. Dettman¹, Lucas Parreiras¹, David S. Guttman⁴, Aviv Regev^{2,3,5,7}, and Linda M. Kohn^{1,7}

¹ Centre for the Analysis of Genome Function and Departments of Cell & Systems Biology and Ecology & Evolutionary Biology, University of Toronto, Mississauga, Ontario L5L 1C6 Canada

² Department of Biology, Massachusetts Institute of Technology, Cambridge, MA, 02140

³ Broad Institute of MIT and Harvard, 7 Cambridge Center, Cambridge MA, 02142

⁴ Centre for the Analysis of Genome Function and Evolution, University of Toronto, Toronto, Ontario M5S 3G5 Canada

⁵ Howard Hughes Medical Institute

Summary

Divergent adaptation can be associated with reproductive isolation in the process of speciation [1]. We recently demonstrated the link between divergent adaptation and the onset of reproductive isolation in experimental populations of the yeast *Saccharomyces cerevisiae* evolved from a single progenitor in either a high-salt or a low-glucose environment [2]. Here, we used whole-genome re-sequencing of representatives of three populations to identify 17 candidate mutations, six of which explained the adaptive increases in mitotic fitness in the two environments. In two populations evolved in high salt, two different mutations occurred in the proton efflux pump gene *PMA1* and the global transcriptional repressor gene *CYC8*; the *ENA* genes encoding sodium efflux pumps were over-expressed once through expansion of this gene cluster and once due to mutation in the regulator *CYC8*. In the population from low glucose, one mutation occurred in *MDS3*, which modulates growth at high pH, and one in *MKT1*, a global regulator of mRNAs encoding mitochondrial proteins, the latter recapitulating a naturally-occurring variant. A Dobzhansky-Muller (DM) incompatibility between the evolved alleles of *PMA1* and *MKT1* strongly depressed fitness in the low-glucose environment. This DM interaction is the first reported between experimentally evolved alleles of known genes and shows how reproductive isolation can arise rapidly when divergent selection is strong.

To whom correspondence should be addressed: jb.anderson@utoronto.ca and aregev@broad.mit.edu.

⁶These authors contributed equally to this work.

⁷These authors contributed equally to this work.

Publisher's Disclaimer: This is a PDF file of an unedited manuscript that has been accepted for publication. As a service to our customers we are providing this early version of the manuscript. The manuscript will undergo copyediting, typesetting, and review of the resulting proof before it is published in its final citable form. Please note that during the production process errors may be discovered which could affect the content, and all legal disclaimers that apply to the journal pertain.

Results

Incipient speciation during yeast experimental evolution in high salt and low glucose

Divergent adaptation of populations may be associated with the evolution of reproductive isolation in two different ways: ecological isolation [3,4] and Dobzhansky-Muller (DM) interaction [5]. Under ecological isolation, populations adapt to divergent environments through the accumulation of genetic changes that result in increased fitness. If formed, hybrid populations are genotypically intermediate and therefore sub-optimally matched to any environment in which adaptation occurred. Reduced fitness in hybrids retards, if not prevents, gene flow between populations, contributing to speciation. With DM interaction, there is negative epistasis in hybrids among alleles that have never been tested together by natural selection. Ecological isolation and DM interaction can independently contribute to speciation.

Among fully-fledged species, the majority of genes identified as components of DM interactions are unrelated to adaptation [6]. An exception is the DM interaction between a nuclear gene *AEP2* in *Saccharomyces bayanus* and a mitochondrial gene *OL11* in *S. cerevisiae* [7]. It is unknown whether any of the DM incompatibilities identified to date among existing species drove the ancient speciation events.

To separate initial events from subsequent evolutionary change in extant species, we focused on the earliest mutations conferring adaptation and reproductive isolation in experimental populations of yeast under strongly divergent selection. We studied experimental populations of *S. cerevisiae* that evolved from a single progenitor (**P**) in either a high-salt (**S**) or a low-glucose (**M**) environment [2]. These populations were propagated as batch-transferred cultures with population size fluctuating daily between 10^6 ('bottleneck size') and 10^8 individuals. We then demonstrated that fitness reduction in hybrids in this system had origins both in ecological isolation and in DM interaction. Our study [2] required only 500 generations of divergent evolution from a common ancestor. This short time frame is in contrast to other studies of genes involved in speciation [5–10] and of isolating mechanisms among extant species [11–13].

Next-generation sequencing of progenitor and evolved strains identifies seventeen candidate mutations

To identify the evolved mutations, we conducted whole-genome re-sequencing of single haploid representatives from two populations evolved in high salt (**S2** and **S6**), one population evolved in low glucose (**M8**), and their common progenitor (**P**). The three evolved strains had increased fitness in the respective environments in which they evolved (Figure S1). We mapped all sequenced reads to the finished *S. cerevisiae* S288C genome, and located mutations unique to each evolved strain (Supplemental Experimental Procedures).

Seventeen candidate mutations were confirmed by PCR, conventional sequencing, and comparative genome hybridization analysis (Tables S1 and S2). These included: in **S2**, non-synonymous point mutations in the coding sequence of *PMA1*, *GCD2*, *MET3*, and *LAP2*, a point mutation in the intergenic region 3' to *SEC13* and *PNP1*, and an expansion of the *ENA* gene cluster; in **S6**, non-synonymous point mutations in the *PMA1* and *CYC8* coding sequences, point mutations in the *YBP2* and *CAB3* promoters, and a contraction of the *ASP3* gene cluster; and in **M8**, non-synonymous mutations in the coding sequences of *TIM11*, *RPH1*, *MDS3*, *MKT1*, and *SGT1*, and a synonymous mutation in *UBI4*. We note that two other studies have identified mutations in genome-wide screens from experimental yeast populations [14, 15].

Assessing the contribution of each evolved allele to fitness in the adaptive environment

To assess the contribution of these mutations to adaptation, we measured the fitness effects of each of the mutations unique to **S2**, **S6**, and **M8** (Tables S1 and S3–S7) by monitoring culture

density during growth (Supplemental Experimental Procedures). We compared the fitness of the progenitor (**P**) and evolved (**S2**, **S6**, and **M8**) strains, in both high-salt and low-glucose environments, to that of progeny genotyped for all the identified mutations from crosses with the progenitor (**S2** × **P**, **S6** × **P**, Figure 1, and **M8** × **P**, Figure 2), and between the evolved strains (**S2** × **M8** and **S6** × **M8**, Figure 5, Figures S1 and S2, see Tables S3–S7 for all genotypes and fitness measurements). To control for variation between experiments, we normalized each measurement by the fitness of the progenitor as a reference (the fitness value of the progenitor is 1.0 in all graphs). We used 2-way ANOVA (linear, additive model) to test for the fitness effect of each evolved and ancestral allele and for interactions between every pair of alleles ($P < 0.05$, Bonferroni multiple hypothesis correction; Supplemental Experimental Procedures, Table S8). Since several of the candidate SNPs involved regulatory genes (the general transcription factor *CYC8* in **S6** and the chromatin modifier *RPH1* and the RNA regulatory protein *MKT1* in **M8**), we also profiled the expression of each of the progenitor and evolved strains in YPD, high-salt and low-glucose (Figure 3).

Recurrent mutations in *PMA1*, and phenocopy mutations in *ENA* and *CYC8* contribute the majority of the observed fitness effects in high salt

Analysis of the 48 **S2** × **P** progeny showed that the main adaptive determinants for the higher fitness of **S2** in salt are the *ENA* gene-cluster expansion (mean fitness relative to progenitor: *ENAIe* segregants – 2.35, *ENAIa* segregants – 1.54, $P < 0.008$) and the evolved allele of *PMA1* (mean fitness relative to progenitor: *PMAIe* segregants – 3.03 *ENAIa* segregants – 1.16, $P < 10^{-4}$), with the *PMA1* allele having a more pronounced effect (Figure 1A and Table S3). *PMA1* encodes an essential ATP-driven proton pump responsible for maintaining the pH gradient across the cell membrane [16], and the *ENA* genes encode three paralogous ATP-driven sodium efflux pumps [17] (a similar *ENA* gene-cluster expansion has been observed previously [18] with adaptation to high salt). *ENA* and *PMA1* also had the only significant additive interaction (ANOVA, $P < 10^{-4}$, Figure 1C), although this interaction was only marginally significant on a logarithmic scale (ANOVA of $\log(\text{fitness})$, $P < 0.07$). Nevertheless, the individual effects of the evolved alleles of *ENA* and *PMA1* in increasing fitness act in an unreduced (non-interfering) manner when together in the same haploid genotype. This is consistent with a reduction of H⁺ efflux associated with the evolved allele of *PMA1*, and a greater Na⁺ efflux by the expanded *ENA* gene cluster. Together, the evolved allele of *PMA1* and the *ENA* expansion conferred nearly the full fitness increase of the **S2** haploid over the progenitor. Subsidiary minor effects of other mutations are summarized in Table S1.

S6 revealed a pattern of adaptation remarkably parallel to that of **S2** (Figure 1B and Table S4). A mutation in *PMA1* distinct from that in **S2** and another in *CYC8*, a general transcriptional repressor that acts together with *TUPI*, each conferred large gains in fitness (mean fitness relative to progenitor: *PMAIe* segregants – 2.40; *PMAIa* segregants – 1.64, $P < 0.002$; *CYC8e* segregants – 2.68; *CYC8a* segregants – 1.39, $P < 10^{-4}$). A pairwise interaction between *PMA1* and *CYC8* (Figure 2D), was positive and marginally significant on an additive scale (ANOVA, $P < 0.0074$, significance threshold of $P = 0.0083$ with 6 comparisons), but not on a logarithmic scale ($P < 0.023$, significance threshold of $P = 0.0083$ with 6 comparisons). The fitness effects of the evolved alleles of *PMA1* and *CYC8* are non-interfering when together in the same haploid genotype. The growth defect of **S6** (Figure S1A and B) was due to the mutation in *PMA1*; all genotyped strains with the evolved allele grew poorly in YPD and in low glucose (Figure S1G).

The cluster of genes whose expression is specifically induced in **S6** (Figure 3B) is enriched for targets of the Tup1-Cyc8 complex (140 common genes between 837 Tup1-Cyc8 targets and 240 genes in the **S6** up-regulated cluster, out of 5728 genes in array, $P < 1.5 \times 10^{-58}$), suggesting that the evolved *CYC8* allele encodes a less potent transcriptional repressor than the ancestral

allele. Furthermore, these genes – repressed by Tup1-Cyc8 in YPD [19] and specifically induced in **S6** – are enriched for known genes induced in the osmotic stress response [20] (53 common genes between 259 OSR genes and 240 genes in the **S6** up-regulated cluster out of 5728 genes in array, $P < 1.52 \times 10^{-23}$). Among the Tup1-Cyc8 target genes that are de-repressed in **S6** are the glycerol biosynthesis enzyme *HOR2* (important for high salt tolerance) and the *ENA1* and *ENA2* genes, phenocopying the effect of the genetic expansion of the *ENA* cluster in **S2**.

Mutations in *MKT1* and *MDS3* contribute to increased fitness in distinct growth phases in low-glucose

The contribution of the **M8** evolved alleles to increased fitness and reproductive isolation in low-glucose depended on growth phase (Figure 2 and Table S5). At 20 h, when the cultures were growing exponentially by fermentation, only the *MDS3* allele conferred a significant fitness advantage (mean fitness relative to progenitor: *MDS3e* segregants – 1.3; *MDS3a* segregants – 0.99, $P < 0.003$) among the **M8** × **P** offspring (Figure 2A), and there were no significant allele interactions. *MDS3* is necessary for growth under alkaline conditions [21], consistent with the fitness benefit it conferred when culture pH was highest (near neutrality). In contrast, the evolved allele of *MKT1* – a major regulator of the mRNAs encoding mitochondrial proteins [22] – conferred a fitness disadvantage at this phase (mean fitness relative to progenitor: *MKT1e* segregants – 0.83; *MKT1a* segregants – 1.36, $P < 10^{-4}$). The effect of each of these alleles was reversed after the diauxic shift from fermentation to respiration (30h, Figure 2B), when the evolved *MDS3* allele conferred a fitness disadvantage (mean fitness relative to progenitor: *MDS3e* segregants – 0.82; *MDS3a* segregants – 1.12, $P < 10^{-4}$) and the evolved *MKT1* allele was nearly neutral (mean fitness relative to progenitor: *MKT1e* – segregants 1.00; *MKT1a* – 0.97).

To explore the stage-dependent effects of *MDS3* and *MKT1*, we used 24 genotyped offspring of two crosses (three tetrads from each cross) segregating only for the evolved and ancestral alleles of *MDS3* and *MKT1* and for no other evolved SNPs. The evolved allele of *MKT1* alone showed no deficit relative to the progenitor in early time points (Figure 3C and 5C), but had a strong increase in fitness late in the growth cycle. This is in contrast to the aggregate effect of *MKT1* in the presence of other segregating SNPs (Figures 3A and B), where we found a fitness deficit early and near neutrality late. Nevertheless, in both experiments, the effect of *MKT1e* had the same directionality: it performs better late in the growth cycle than early. The evolved allele of *MDS3* showed the opposite directionality, performing better early than late. Importantly, genotypes carrying only the evolved alleles of both *MDS3* and *MKT1* closely approximated the growth curve of the **M8** haploid strain, accounting for the adaptation observed in low glucose (Figure 2C).

A competitive fitness assay over a 24 h period provided a third, independent, measure of the individual fitness effects in low glucose of the evolved alleles of *MDS3* and *MKT1*. This period matched the daily batch-culture regimen in the original 500 generation experiment [2], which included both fermentative and respirative energy production. Each mutation conferred a fitness advantage over the progenitor alleles (*MDS3*, 1.25 ± 0.1 SE $n = 9$ and *MKT1* 1.10 ± 0.2 SE $n = 6$). We conclude that our experimental regimen selected for alleles conferring advantages at distinct phases of the yeast growth cycle.

Finally, the evolved alleles of the mitochondrial protein *TIM11* and the chromatin modifier gene *RPH1* conferred smaller, non-significant growth increases at 30h (post-shift, Figure 2B, Tables S5 and S8). This effect is consistent with the role of the *RPH1* paralog in regulating gene expression post-diauxic shift [23]. However, the evolved *RPH1* allele was not essential to reconstitute the full **M8** phenotype.

The *MKT1* allele reverted to a wild allele during experimental evolution

The evolved *MKT1* allele of **M8** is identical to the allele (89G) observed in strains of *S. cerevisiae* of diverse environmental origin and of *S. paradoxus* [24], leading to a non-conservative amino acid change from aspartate (**P**) to glycine (**M8**). *MKT1* encodes a major component in the interaction between Puf3, a sequence-specific RNA binding protein targeting mRNAs involved in mitochondrial function, and P-bodies, which control sequestration and expression of certain mRNAs [22]. The cluster of genes of elevated expression in **M8** strains (Figure 3C) is highly enriched for mitochondrial genes (62 common genes between 588 mitochondrial genes and 90 genes in the **M8** upregulated cluster out of 5728 genes in array, $P < 2.7 \times 10^{-41}$), including aerobic respiration genes (10 common genes between 64 aerobic respiration genes and 90 genes in the **M8** upregulated cluster out of 5728 genes in array, $P < 4.2 \times 10^{-8}$), and in particular known Puf3 targets (59 common genes between 137 Puf3 target genes and 90 genes in the **M8** upregulated cluster out of 5728 genes in array, $P < 9.7 \times 10^{-79}$). Furthermore, the **M8** cluster includes genes more highly expressed in the vineyard strain RM-11 than the lab strain BY (Figure 3C, bottom). The eQTLs for these genes were previously found to be closely linked to the *MKT1* allele that segregates in the BY X RM-11 cross [22].

Taken together, the data suggest a past mutation from the allele (89G) uniformly present in wild strains to that of the laboratory standard (89A), carried by our **P** strain, followed by an exact reversion of that mutation at some point during the 500 generations of evolution from **P** to **M8**. Thus, the progenitor (**P**) laboratory reference strain carries a less potent form of *MKT1*, with lower expression of target genes, strongly selected for in lab experiments focusing on early or mid-log phase cells in which the wild allele (here the “evolved *MKT1*”) confers a growth disadvantage. In contrast, the low-glucose selection regimen on a 24h batch-transfer cycle used in this study may more closely approximate natural conditions in which growth more often approaches stasis, a condition that would favor the reversion to the naturally-occurring 89G allele, and corresponding higher expression of gene targets.

A DM Interaction between *PMA1* and *MKT1*

We next tested for the presence of DM interactions, defined as genetic incompatibilities between alleles independently evolved in the two environments. We measured the fitness, in the two selective environments, of 96 offspring from 24 tetrads from the **S2** × **M8** and **S6** × **M8** crosses (Figures S1 and S2). All progeny were fully genotyped for all segregating SNPs, gene-cluster size alterations, and mating type, all of which segregated ~1:1 in tetrads (Tables S6 and S7). As before, we tested each pairwise combination of loci for interaction by means of ANOVA (Table S8).

Among the offspring of the **S2** × **M8** cross in the low-glucose environment at 24 hours (Figure 4A and Supplemental Table 6), we found only one marginal P-value of 0.015 for a *PMA1e-MKT1e* negative fitness interaction (in the presence of other segregating alleles). Since the initial value was marginal, we tested this preliminary evidence for an interaction in two additional independent experiments.

In the first, we measured the fitness of 24 genotyped offspring of two crosses (three tetrads from each cross), that segregated at **only** the two SNP sites in *PMA1* and *MKT1* (no other evolved alleles were present in the cross). Here, we found that the fitness of offspring carrying both evolved alleles was depressed over the entire growth cycle in low glucose (Figure 4B), most prominently at the 21 and 24h time points (the same time point as in Figure 4A). At 24h, an overall ANOVA of additive variation over the four genotypes was statistically significant ($P < 0.016$, one test only) and a Tukey-Kramer HSD test indicated that the only difference was between the *PMA1a MKT1e* and *PMA1e MKT1e* genotypes. The reduction in the *PMA1e MKT1e* genotype is therefore due to the presence of the *PMA1e* allele, which is otherwise

nearly neutral in the low-glucose environment and closely tracks the progenitor over the entire growth cycle. We further confirmed this result in three additional replicate experiments with the same strains at 24h, finding a significant interaction between the *PMA1* and *MKT1* alleles, when fitting a linear mixed model treating strain as a random effect and tested against a null model of no interaction between *PMA1* and *MKT1* ($PMA1aMKT1a$: 0.69 ± 0.02 , $PMA1aMKT1e$: 0.70 ± 0.02 , $PMA1eMKT1a$: 0.66 ± 0.01 , $PMA1eMKT1e$: 0.46 ± 0.03 , $P < 10^{-4}$). This interaction is also significant on log scale ($P < 4 \times 10^{-5}$). This fulfills the criterion for a DM interaction [2]. Similar assays with offspring segregating for *MDS3* and *PMA1* showed no such negative interaction (Figure 4C).

We independently confirmed the negative interaction between the *PMA1* and *MKT1* genotypes in competition experiments in the low-glucose environment at an early time point (17h under conditions matching those in Figure 4B), showing a negative reduction in the number of doublings in the *PMA1e MKT1e* genotype strain ($MKT1e$, 0.87 ± 0.01 SE (n=3); $PMA1e$, 0.89 ± 0.02 SE (n=3); $PMA1e MKT1e$, $0.7 \pm .07$ SE (n=3) all relative to the doublings by the progenitor). As a control, we confirmed the expected beneficial effect of *MDS3e* in the competition assay ($1.28 + 0.01$ SE (n=2)). The difference in fitness among the genotypes fell just short of significant ($P < 0.061$, one-way ANOVA, linear scale), likely reflecting the smaller sample size and the earlier (17h) time point. Nevertheless, each of these three experiments supported the conclusion of negative interaction between the evolved alleles of *PMA1* and *MKT1*, most notably at 24h. In contrast, there was no evidence for a DM interaction in the **S2** × **M8** and **S6** × **M8** offspring in high salt and the **S6** × **M8** offspring in low glucose (Supplemental S7 and S8), where all adaptive determinants had effects similar to those in crosses of the evolved strains and the progenitor (Figures S1A and B).

Discussion

In this study we used whole-genome sequencing of progenitor and evolved strains, along with genotyping, fitness assays, and mRNA profiling to identify and characterize the genetic and molecular basis of early events associated with divergent selection in experimental yeast populations. We found six key determinants, each of which contributes to ecological isolation in which genotypically mixed hybrids are not as well matched to either environment as the pure evolved strains.

The DM interaction between *PMA1* and *MKT1* is the first reported between evolved alleles of known genes in experimental populations derived from a common ancestor. Although it is tempting to speculate on how such an incompatibility might affect natural yeast populations, our study was limited to haploid effects. One possibility is that a DM incompatibility like that reported here would quickly be eliminated with recombination. Conversely, such a DM interaction might present a strong reproductive isolation mechanism in nature under the low rate of outcrossing in *S. cerevisiae* [26]; in such a case the incompatibility would persist in hybrid populations. These possibilities remain to be investigated.

No consistent functional theme has yet emerged among the known “speciation genes” implicated in DM interactions among species in nature [5–10]. Here, we show that the adaptive mechanisms evolved in response to strong directional selection in two environments have substantial effects on gene regulation and phenotype and that at least two of the adaptive determinants produce an intrinsic clash resulting in a fitness reduction characteristic of a DM interaction. In extant species examined to date, the majority of DM incompatibilities occur in genes unrelated to ecological adaptation [6]. Our study, in which we experimentally set the conditions thought to foster incipient speciation, documents a counter example in which divergent adaptive changes themselves confer a DM incompatibility. It is possible that newly evolved adaptive mechanisms under other conditions will have similarly far-reaching

consequences, with potential for DM incompatibility. We propose that the potential pool of speciation genes includes genes conveying adaptation under strong selection in the earliest stages of speciation – that functional diversity in speciation genes could reflect the diversity of adaptive mechanisms.

Highlights

- Incipient speciation in experimental yeast populations investigated by genome sequencing and genetics.
- Specific changes underlying adaptation recur in independently-evolved strains.
- Mutations have substantial effects on gene expression programs.
- Newly-evolved Dobzhansky-Muller (DM) incompatibility reduces the fitness of hybrids.

Supplementary Material

Refer to Web version on PubMed Central for supplementary material.

Acknowledgments

J.B.A. and L.M.K. were supported by Discovery Grants from the Natural Sciences and Engineering Research Council of Canada. We thank the Broad Sequencing Platform, and in particular H. Spurling, for sequencing work, and I. Gat-Viks, M. Chan, J. Konieczka, D. Mohammad, C. Ye, M. Guttman, and other members of the Regev lab for helpful discussions and comments. J.F. was supported by the NSF Graduate Research Fellowship, D.A.T. was supported by the Human Frontiers Science Program, A.R. was supported by the Howard Hughes Medical Institute, a Career Award at the Scientific Interface from the Burroughs Wellcome Fund, an NIH PIONEER award, and a Sloan Fellowship.

References

1. Coyne, JA.; Orr, HA. Speciation. Sunderland: Sinauer; 2004.
2. Dettman JR, Sirjusingh C, Kohn LM, Anderson JB. Incipient speciation by divergent adaptation and antagonistic epistasis in yeast. *Nature* 2007;447:585–588. [PubMed: 17538619]
3. Rundle HD, Nosil P. Ecological speciation. *Ecology Letters* 2005;8:336–352.
4. Schluter D. Evidence for ecological speciation and its alternative. *Science* 2009;323:737–741. [PubMed: 19197053]
5. Wu CI, Ting CT. Genes and speciation. *Nat Rev Genet* 2004;5:114–122. [PubMed: 14735122]
6. Presgraves DC. The molecular evolutionary basis of species formation. *Nat Rev Genet* 11:175–180. [PubMed: 20051985]
7. Lee HY, Chou JY, Cheong L, Chang NH, Yang SY, Leu JY. Incompatibility of nuclear and mitochondrial genomes causes hybrid sterility between two yeast species. *Cell* 2008;135:1065–1073. [PubMed: 19070577]
8. Brideau NJ, Flores HA, Wang J, Maheshwari S, Wang X, Barbash DA. Two Dobzhansky-Muller genes interact to cause hybrid lethality in *Drosophila*. *Science* 2006;314:1292–1295. [PubMed: 17124320]
9. Sweigart AL, Mason AR, Willis JH. Natural variation for a hybrid incompatibility between two species of *Mimulus*. *Evolution* 2007;61:141–151. [PubMed: 17300433]
10. Tang S, Presgraves DC. Evolution of the *Drosophila* nuclear pore complex results in multiple hybrid incompatibilities. *Science* 2009;323:779–782. [PubMed: 19197064]
11. Delneri D, Colson I, Grammenoudi S, Roberts IN, Louis EJ, Oliver SG. Engineering evolution to study speciation in yeasts. *Nature* 2003;422:68–72. [PubMed: 12621434]
12. Greig D. Reproductive isolation in *Saccharomyces*. *Heredity* 2009;102:39–44. [PubMed: 18648383]
13. Liti G, Barton DB, Louis EJ. Sequence diversity, reproductive isolation and species concepts in *Saccharomyces*. *Genetics* 2006;174:839–850. [PubMed: 16951060]

14. Gresham D, Desai MM, Tucker CM, Jenq HT, Pai DA, Ward A, DeSevo CG, Botstein D, Dunham MJ. The repertoire and dynamics of evolutionary adaptations to controlled nutrient-limited environments in yeast. *PLoS Genet* 2008;4:e1000303. [PubMed: 19079573]
15. Lynch M, Sung W, Morris K, Coffey N, Landry CR, Dopman EB, Dickinson WJ, Okamoto K, Kulkarni S, Hartl DL, et al. A genome-wide view of the spectrum of spontaneous mutations in yeast. *Proc Natl Acad Sci U S A* 2008;105:9272–9277. [PubMed: 18583475]
16. Morsomme P, Slayman CW, Goffeau A. Mutagenic study of the structure, function and biogenesis of the yeast plasma membrane H(+)-ATPase. *Biochim Biophys Acta* 2000;1469:133–157. [PubMed: 11063881]
17. Benito B, Garcia-deblas B, Rodriguez-Navarro A. Potassium- or sodium-efflux ATPase, a key enzyme in the evolution of fungi. *Microbiology* 2002;148:933–941. [PubMed: 11932440]
18. Gerstein AC, Chun HJ, Grant A, Otto SP. Genomic convergence toward diploidy in *Saccharomyces cerevisiae*. *PLoS Genet* 2006;2:e145. [PubMed: 17002497]
19. Hughes TR, Marton MJ, Jones AR, Roberts CJ, Stoughton R, Armour CD, Bennett HA, Coffey E, Dai H, He YD, et al. Functional discovery via a compendium of expression profiles. *Cell* 2000;102:109–126. [PubMed: 10929718]
20. Capaldi AP, Kaplan T, Liu Y, Habib N, Regev A, Friedman N, O’Shea EK. Structure and function of a transcriptional network activated by the MAPK Hog1. *Nat Genet* 2008;40:1300–1306. [PubMed: 18931682]
21. Davis DA, Bruno VM, Loza L, Filler SG, Mitchell AP. *Candida albicans* Mds3p, a conserved regulator of pH responses and virulence identified through insertional mutagenesis. *Genetics* 2002;162:1573–1581. [PubMed: 12524333]
22. Lee SI, Dudley AM, Drubin D, Silver PA, Krogan NJ, Pe’er D, Koller D. Learning a prior on regulatory potential from eQTL data. *PLoS Genet* 2009;5:e1000358. [PubMed: 19180192]
23. Pedruzzi I, Burckert N, Egger P, De Virgilio C. *Saccharomyces cerevisiae* Ras/cAMP pathway controls post-diauxic shift element-dependent transcription through the zinc finger protein Gis1. *EMBO J* 2000;19:2569–2579. [PubMed: 10835355]
24. Liti G, Carter DM, Moses AM, Warringer J, Parts L, James SA, Davey RP, Roberts IN, Burt A, Koufopanou V, et al. Population genomics of domestic and wild yeasts. *Nature* 2009;458:337–341. [PubMed: 19212322]
25. Tirosh I, Reikhav S, Levy AA, Barkai N. A yeast hybrid provides insight into the evolution of gene expression regulation. *Science* 2009;324:659–662. [PubMed: 19407207]
26. Ruderfer DM, Pratt SC, Seidel HS, Kruglyak L. Population genomic analysis of outcrossing and recombination in yeast. *Nat Genet* 2006;38:1077–1081. [PubMed: 16892060]

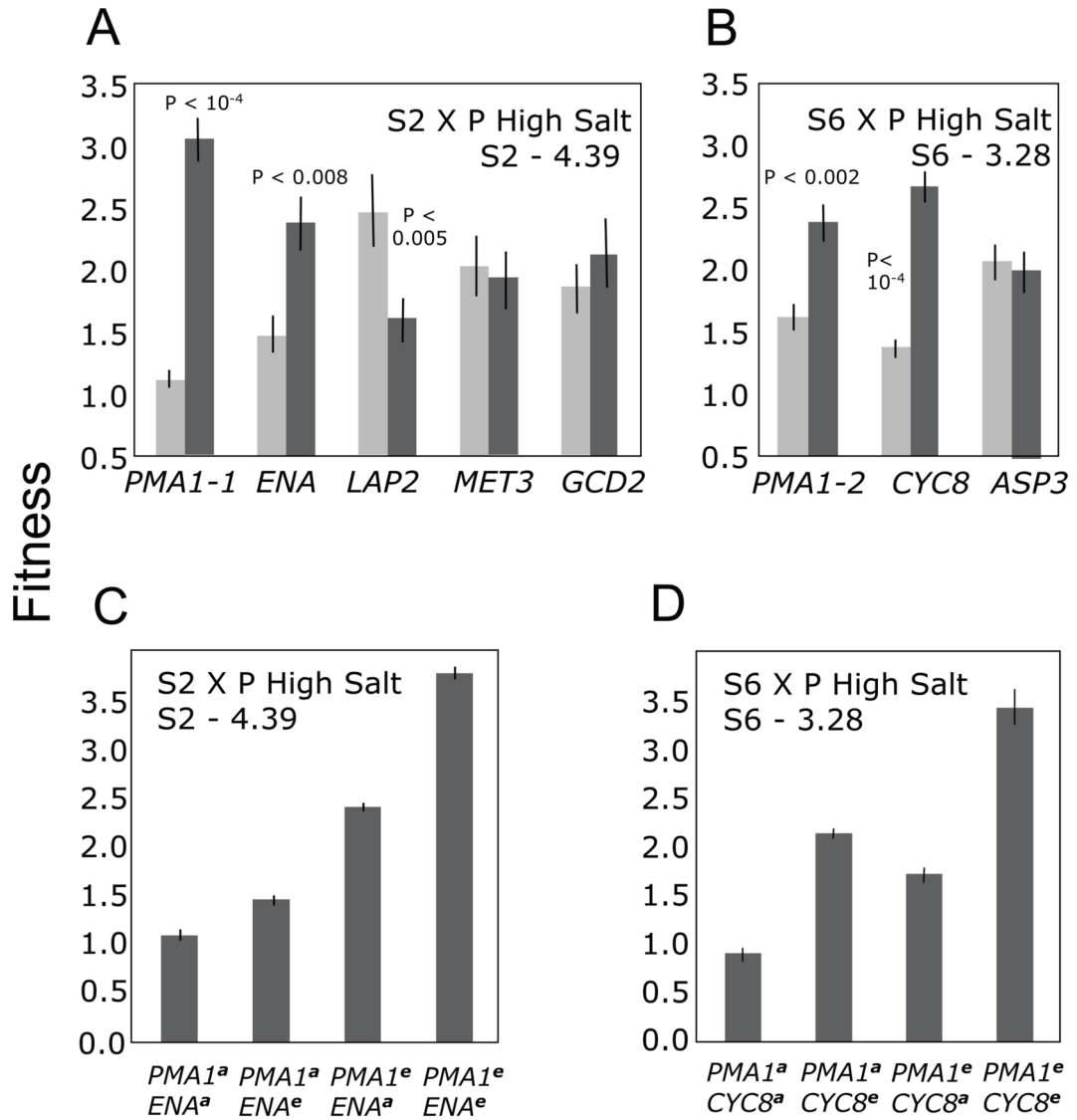


Figure 1. Contribution of S2 and S6 evolved alleles to fitness in high salt

Shown are fitness measurements (OD_{600} , mean and standard error, normalized to the progenitor value) for 48 offspring fully genotyped for all coding alleles identified by sequencing – from each of the crosses **S2** × **P** (**A**, **C**, 5 loci) and **S6** × **P** (**B**, **D**, 3 loci). Data are aggregated by specific alleles as marked (in each marked category, e.g. “*PMA1-2*”, the other alleles are segregating). Full data (including intergenic loci) are available in Tables S3 and S4. (**A**, **B**). The bars represent the average fitness effect of each variant across all offspring. Light gray bars, ancestral alleles; dark bars, evolved alleles. Fitness of evolved parent is shown at the upper right corner. Significant differences are noted with *P*-value. (**C**, **D**) Average pairwise effects of the two most advantageous mutations in each strain. Shown are the same data as in **A** and **B**, but averaged for two-locus genotypes showing positive interaction. Superscript *a* = ancestral allele; superscript *e* = evolved allele. Interaction was tested by ANOVA; all *P* values appear in Table S8.

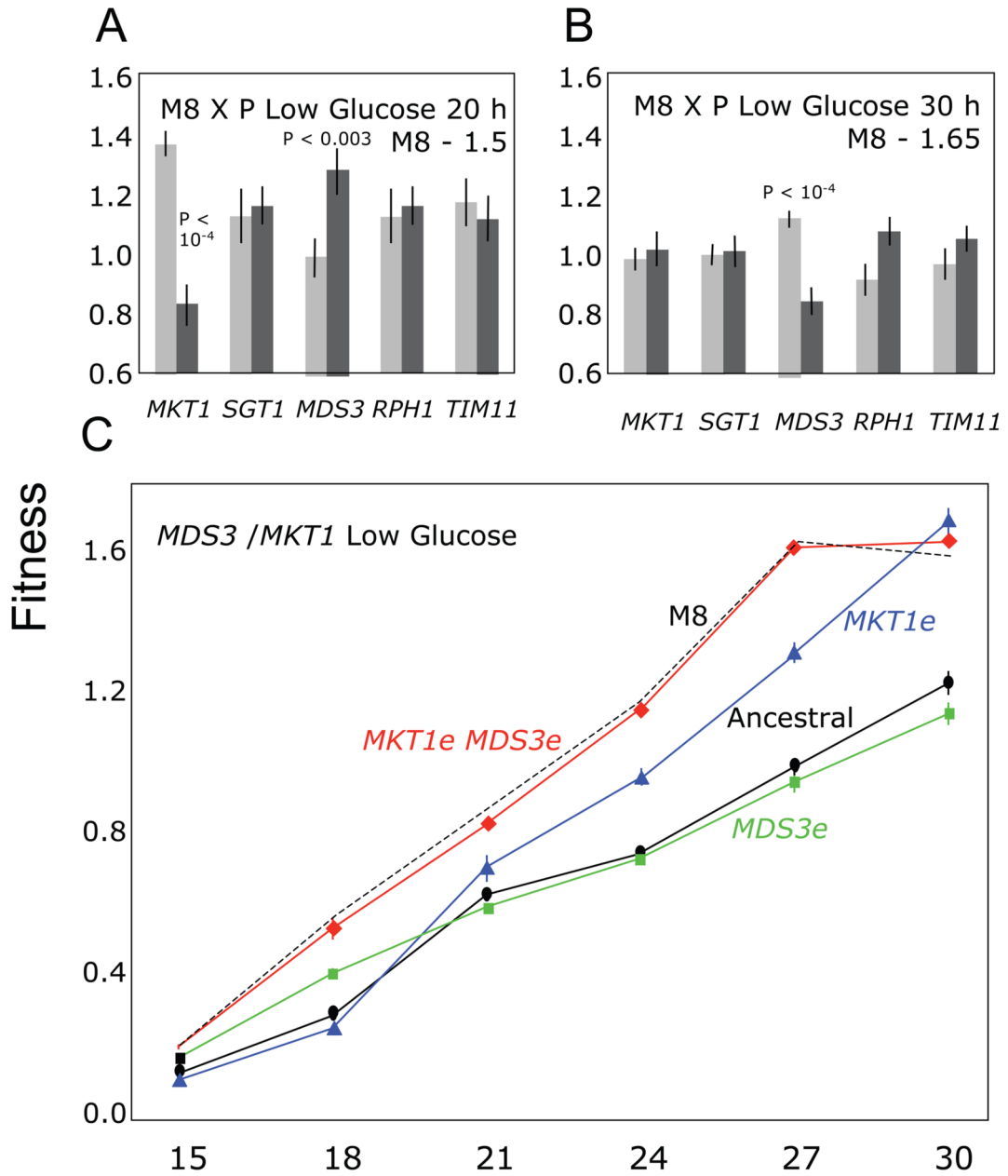


Figure 2. Contribution of M8 evolved alleles to fitness in low glucose

(A, B) Average fitness effect of each variant across the segregant offspring at log-phase (20h) and post-diauxic shift (30h) during growth in low-glucose. Shown are fitness measurements (OD_{600} , mean and standard error, normalized to the progenitor value) for 48 progeny from an M8 × P cross – fully genotyped for all five coding loci identified by sequencing, at 20h (A) and 30h (B) of growth on glucose. Data are aggregated by specific alleles, as marked (in each marked category, e.g. “MKT1”, the other alleles are segregating). Full data are available in Table S5. Light gray bars, ancestral alleles; dark bars, evolved alleles. Fitness of evolved parent is shown at the upper right corner. Significant differences are noted with P-value. All P values appear in Table S8. (C) Evolved alleles of *MDS3* and *MKT1* (*MDS3e* and *MKT1e*) account for the M8 phenotype. Shown are growth curves (OD_{600}) from three tetrads from each of two

independent crosses segregating for *MDS3* and *MKT1*, and no other evolved alleles (based on full genotyping). The number of replicates for each time course varied between four and eight, reflecting independent assortment. The evolved allele of *MDS3* (green) confers a benefit early, while that of *MKT1* (blue) confers a benefit late in the growth cycle, relative to the ancestral genotype (black). Together these two alleles produce a phenotype (red) that matches that of the M8 strain (dashed).

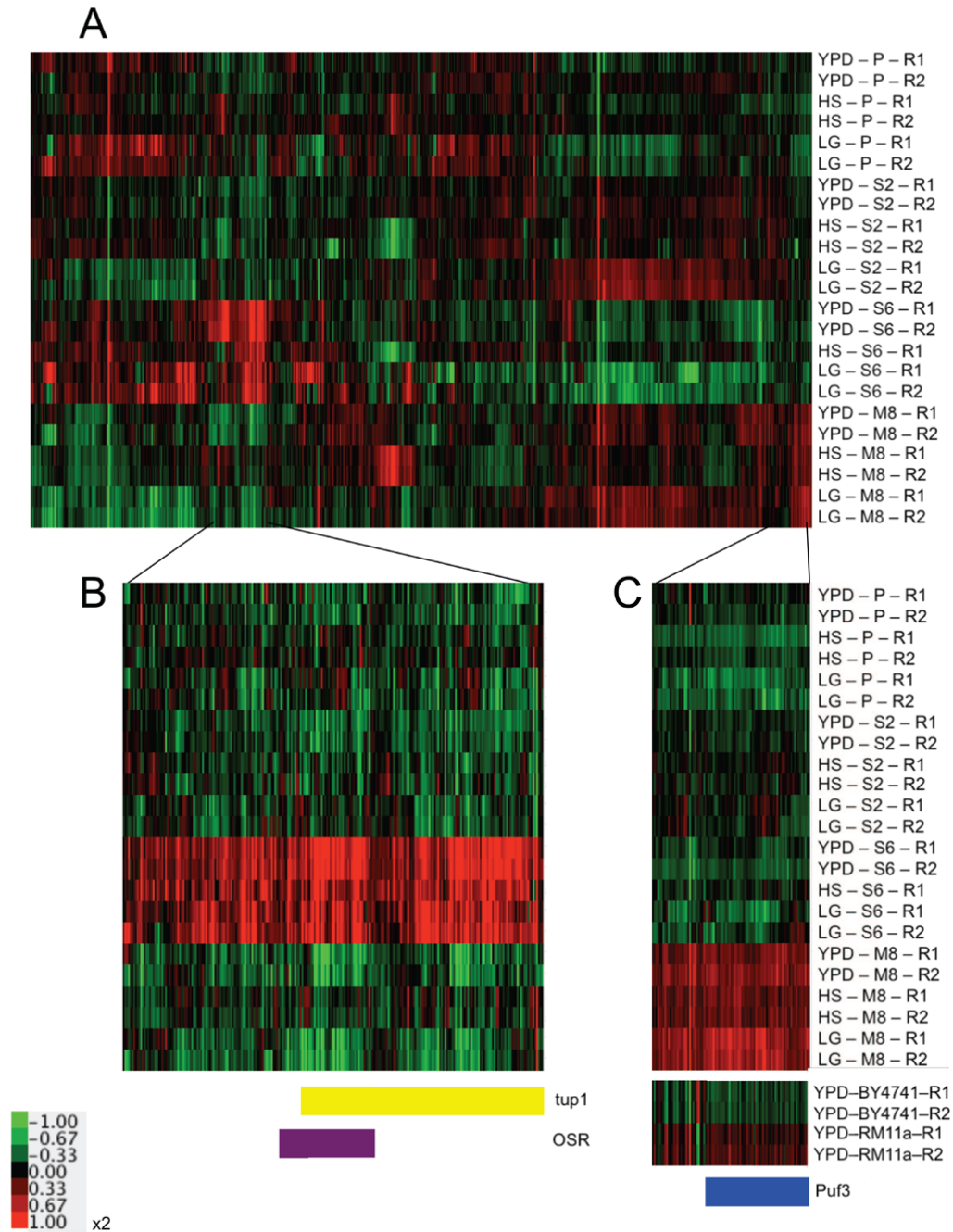


Figure 3. Global expression changes in evolved strains associated with the adaptive genetic changes
(A) Genome wide expression profiles from **P**, **S2**, **S6**, and **M8** strains grown in YPD, low glucose (LG), and high salt (HS) environments. Red – induced compared to mean of all strains in that condition; green – repressed compared to mean of all strains in that condition. **(B)** Genes with high expression specific to **S6** across all conditions are enriched for Cyc8-Tup1 targets and for osmotic response genes. Shown is a zoomed in cluster from (A). Yellow bar – genes whose expression is induced in a deletion of the *TUP1* gene [19]; purple bar – genes whose expression is induced during the Osmotic Stress Response (OSR) to high salt [20]. Genes are re-ordered by the *TUP1* and OSR annotations. **(C)** Genes with high expression specific to **M8** across all conditions are induced in the RM-11 wine strain and enriched for Puf3 targets.

Top panel – zoomed in cluster from (A). Bottom panel – expression of the same genes in the laboratory strain BY and in the wild wine strain RM. Blue bar – genes in the Puf3 module [22], whose eQTL in a cross between BY and RM has been linked to the same genetic change in *MKT1* found also in the **M8** strain. Genes are re-ordered by membership in the Puf3 module.

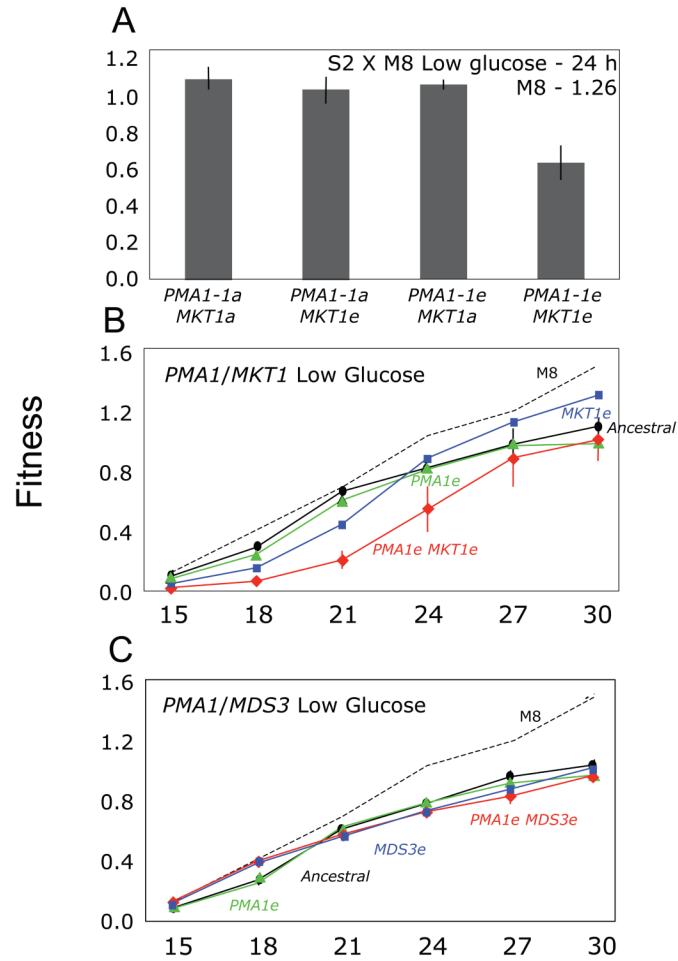


Figure 4. DM interactions between the evolved alleles of *PMAI* and *MKT1*

(A) DM interaction between the evolved alleles of *PMAI* and *MKT1* at 24h in low-glucose. Shown are the fitness measurements (OD₆₀₀, mean and standard error, normalized to the progenitor value) of 96 offspring of a cross between **S2** and **M8** in the low-glucose environment at 24h grouped by their two-locus genotypes for *PMAI* and *MKT1* (*e* - evolved allele; *a* - ancestral allele); note the depressed fitness of the genotype carrying both evolved alleles of these genes. ANOVA: evolved allele of *PMAI*, $P < 10^{-4}$; evolved allele of *MKT1*, $P < 10^{-4}$; and interaction of the evolved alleles of *PMAI* and *MKT1*, $P < 0.015$. Full data are available in Table S6 and all P values of all tests are listed in Table S8. (B) DM interaction between the evolved alleles of *PMAI* and *MKT1* along the growth curve. Shown are growth curves from three tetrads from each of two independent crosses segregating for *PMAI* and *MKT1*, and carrying no other evolved alleles (based on full genotyping). The number of replicates for each time course varied between four and eight, reflecting independent assortment. The genotype carrying the evolved alleles of *PMAI* and *MKT1* (red) shows poor growth at all time points (up to 27h) relative to the other genotypes. The other genotypes are marked as *PMAIe* (green); *MKT1e* (blue); ancestral (*PMAIa* *MKT1a*, black); and M8 (dashed). (C) Absence of an interaction between *PMAI* and *MDS3*; analysis as in B: *PMAIe* (green); *MDS3e* (blue), *PMAIe* *MDS3e* (red); ancestral (*PMAIa* *MDS3a*, black); and M8 (dashed).